

This is an Open Access document downloaded from ORCA, Cardiff University's institutional repository: <https://orca.cardiff.ac.uk/id/eprint/124770/>

This is the author's version of a work that was submitted to / accepted for publication.

Citation for final published version:

Caiti, Massimiliano, Padovan, Daniele and Hammond, Ceri 2019. Continuous production of hydrogen from formic acid decomposition over heterogeneous nanoparticle catalysts: from batch to continuous flow. *ACS Catalysis* 9 (10) , pp. 9188-9198. 10.1021/acscatal.9b01977

Publishers page: <http://dx.doi.org/10.1021/acscatal.9b01977>

Please note:

Changes made as a result of publishing processes such as copy-editing, formatting and page numbers may not be reflected in this version. For the definitive version of this publication, please refer to the published source. You are advised to consult the publisher's version if you wish to cite this paper.

This version is being made available in accordance with publisher policies. See <http://orca.cf.ac.uk/policies.html> for usage policies. Copyright and moral rights for publications made available in ORCA are retained by the copyright holders.



# Continuous production of hydrogen from formic acid decomposition over heterogeneous nanoparticle catalysts: from batch to continuous flow

Massimiliano Caiti, Daniele Padovan and Ceri Hammond\*

Cardiff Catalysis Institute, School of Chemistry, Cardiff University, Cardiff, CF10 3AT, United Kingdom

## Supporting Information Placeholder

**ABSTRACT:** We investigate the continuous generation of hydrogen *via* the low temperature (< 110 °C), additive-free dehydrogenation of formic acid over heterogeneous Pd/C. Through a combination of kinetic (batch and continuous), spectroscopic and mechanistic studies, we develop structure-activity-lifetime relationships for this process, and in doing so reveal that a combination of pore fouling and poisoning by formate ions result in deactivation of the catalyst during continuous operation. Although these factors result in extensive deactivation in Plug Flow mode, promising results can be obtained by minimizing the steady state concentration of formic acid by operating in a Continuous Stirred Tank reactor. In doing so, continuous operation of the system without loss of activity for over 2500 turnovers is achieved, at mild conditions and in the absence of stoichiometric additives.

**Keywords:** Hydrogen production, continuous flow, Pd nanoparticles, catalyst deactivation, hydrogen storage.

## Introduction

Increasing energy demand from a growing population, combined with increasing awareness of the negative impacts of fossil feedstock and climate change phenomena, have pointed out the urgency of developing new ways to produce energy. In this regard, the oxidation of hydrogen by fuel cells (Proton Exchange Membranes, PEM) represents a promising, clean solution, as they generate electricity and produce water as the only by-product.<sup>1-3</sup> They are also particularly suitable as devices for portable electricity generation. However, the source of hydrogen and its method of storage represent two major bottlenecks in this technology. Typically, gaseous hydrogen is compressed and stored in cylinders at high pressure (above 200 bar), making its handling impractical and risky.<sup>4-6</sup> Moreover, industrial hydrogen is almost exclusively produced by steam reforming of natural gas, a finite fossil resource. Electrolytic water splitting is evidently a cleaner source of hydrogen. Yet, despite the abundance of water, this process is currently quite energy inefficient, particularly when non-renewable resources provide the energy to perform water splitting.

As such, much emphasis has recently been placed on the catalytic decomposition of various hydrogen-containing molecules (so-called storage compounds), in particular so that molecular hydrogen can be produced for portable fuel cell devices.<sup>7-8</sup> Amongst a

number of well explored options,<sup>9-14</sup> formic acid (HCOOH) is one of the most promising, given the fact it has a relatively high content of hydrogen (4.4 wt. %), and is a stable liquid at room temperature and pressure.<sup>15-16</sup> Although formic acid is currently produced industrially from fossil resources, there are several recent examples in which it can be obtained by the direct oxidation of biomass at high yields.<sup>17-18</sup> Moreover, it is frequently encountered as by-product in many biomass-based process, such as the hydrolysis of 5-hydroxymethyl furfural. Thus, with the growing scale of biomass processes, there are possibilities of having a large stock of renewable formic acid available in the future.

Over the last decade, the development of catalysts capable of decomposing formic acid to hydrogen has been the topic of much attention. Amongst these, some of the most active are homogeneous in nature, employing active elements such as iridium, ruthenium and rhodium, amongst others.<sup>19-23</sup> Despite their excellent catalytic performances, their solubility and requirement for complex and expensive ligands limits their large-scale practicality.<sup>24-27</sup> However, whilst many heterogeneous catalysts have been studied, many solid catalysts require elevated temperatures (> 250 °C) and gas phase operation, which also limits their practicality.<sup>28</sup> In several cases, homogeneous and heterogeneous catalysts also require the utilisation of stoichiometric equivalents of amines for any catalytic activity to be achieved, evidently undermining their potential.<sup>20-22</sup>

A more favourable approach involves the development of heterogeneous catalysts capable of low temperature formic acid decomposition in the absence of external additives.<sup>29-34</sup> In this regard, supported metallic nanoparticles have been found to be particularly promising in term of selectivity and activity.<sup>35-37</sup> For example, Dimitratos *et al.* have systematically studied the performance of a commercial Pd on carbon catalyst (5 wt. % Pd/C) at mild conditions (30-90 °C), and found this catalyst to be one amongst the best performing in the open literature.<sup>38</sup> However, these studies were performed in batch reactors, which are unable to produce a continuous, stable stream of hydrogen for fuel cell applications. On a scientific level, such reactors also prohibit detailed study of the lifetime of the catalyst, which is often its key performance indicator.<sup>39,40</sup> Accordingly, studies of formic acid decomposition under continuous conditions are an important challenge to determine the true potential of this technology.

In respect to this, a handful of reports have recently set about exploring the decomposition of formic acid under continuous conditions over both homogeneous and heterogeneous catalysts in Continuous Stirred Tank (CSTR) mode.<sup>41-43</sup> Yet, in all of these

previous studies, stoichiometric equivalents of amines were employed. Accordingly, it is clear that no heterogeneous catalyst, capable of the continuous, additive-free dehydrogenation of formic acid at mild conditions, has yet been identified. Moreover, other types of continuous reactors – particularly Plug Flow Reactors (PFRs) – have yet to be explored for this chemistry, despite their widespread utilisation in other branches of the chemical society and the advantages they offer over CSTRs. Finally, on a fundamental level, these previous studies have not focused on the structural and chemical changes that catalysts undergo during this catalytic process. As such, detailed knowledge of the rates of deactivation of catalysts for this reaction, in addition to fundamental knowledge regarding the mechanisms of deactivation, is not available, despite its critical importance.<sup>39,40</sup>

Here, we investigate the continuous production of hydrogen through the decomposition of formic acid over a commercially available Pd/C. Detailed kinetic studies in various reactor modes, including PFR and CSTR, are coupled to a variety of mechanistic and spectroscopic experiments, which permit the generation of structure-activity-lifetime relationships. In addition to providing unique mechanistic insight into this reaction, these studies also allow us to identify routes to mitigate deactivation, and identify the optimal reactor mode from a productivity and stability perspective with which future kinetic studies should be performed.

## Results and Discussion

**Kinetic studies: from batch to continuous.** As described above, we have previously identified commercially available Pd on carbon (5 wt. % Pd/C, henceforth Pd/C) to be a suitable catalyst for the additive free decomposition of formic acid at mild conditions (30-90 °C). In these previous studies, we benchmarked both the selectivity of the catalyst (dehydrogenation vs. dehydration and hence, the concentration of CO produced), in addition to the basic kinetic parameters of the catalyst, and our ability to measure the rates of reaction based both on gas evolution (volumetric displacement) and formic acid consumption (HPLC and <sup>1</sup>H NMR) – an important step considering that different types of continuous reactors require different modes of reaction analysis (see ESI Figure S1). Previous studies on the reusability of the catalyst suggested that Pd/C possess a good degree of stability, since five consecutive uses during ‘recyclability studies’ exhibited less than 5 % of loss of performance between cycles.

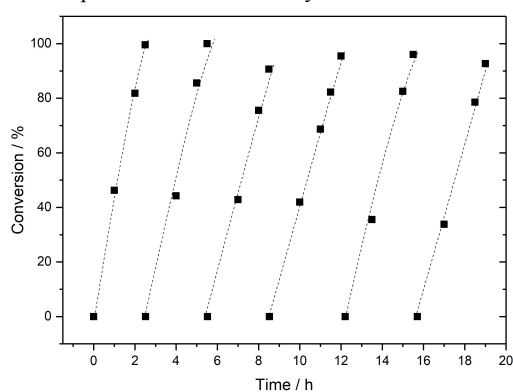


**Figure 1.** Batch tests of formic acid decomposition over Pd/C with fresh aliquots of formic acid periodically added to the reactor without removal of the catalyst or other treatments. Reaction conditions: Pd/C (15 mg), Aqueous formic acid (10 mL, 0.5 M) (formic acid/Pd=100 per cycle), 50 °C, 800 rpm.

Since classical reusability studies can easily over-estimate the potential stability of the catalyst, we commenced our study by extending classical reusability experiments by adding fresh ali-

quots of substrate to a batch reactor once a reaction cycle was completed without removing the catalyst from the reactor between cycles (Figure 1). In this way, perturbation of the catalyst between ‘cycles’ is minimised. Over six ‘cycles’ the catalyst still retained good initial activity, with the rate of reaction observed during the ‘sixth’ cycle being approximately 75 % that of the first.

To better probe catalyst deactivation, kinetic studies in continuous reactors are essential.<sup>39,40</sup> Amongst such reactors, PFRs - in which the catalyst bed is confined inside a tubular column, and the reactant solution is continually pumped over the catalyst bed - offer several advantages, including higher rates of reaction, better temperature control, good mass and excellent heat transfer, and facilitated study of the catalytic material post (and during) reaction by (*in situ*) spectroscopy. Accordingly, evaluation of the deactivation phenomena present in the system was made by analysing the time on stream profile for the conversion of formic acid over Pd/C in a PFR between 30-110 °C. Kinetic relevance of the reactor was verified by confirming the absence of external and internal transport limitations in the required linear velocity range (Figure S2). Comparison of the performance of the catalyst at each temperature was made by determination of its initial activity (initial turnover frequency, TOF<sub>0</sub>, Equation 1) and rate of deactivation (*k<sub>d</sub>*, using the approach of Levenspiel (Figure 2 (Left) inset)). For each catalytic experiment, the contact time (Equation 2) was adjusted in order that each experiment start from a similar level of conversion and hence, the reaction coordinate.<sup>40</sup> Figure 2 (Right) presents the time on stream profiles at different temperatures, and Table 1 summarises the activity (TOF<sub>0</sub>) and stability (*k<sub>d</sub>*) of the catalyst at that temperature.

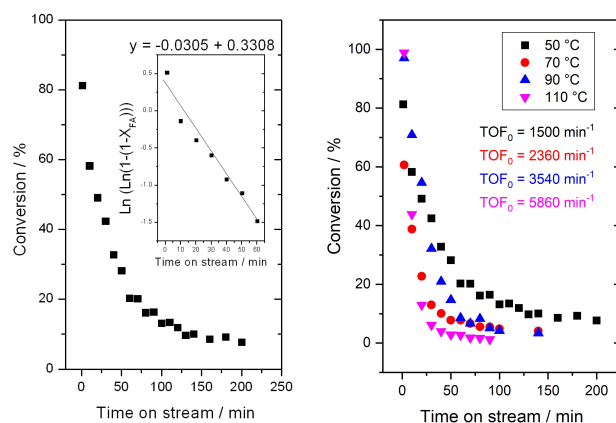


**Figure 2.** (Left) Formic acid conversion as function of time on stream at 50 °C, with the Levenspiel plot to calculated *k<sub>d</sub>* shown in the inset. Reaction conditions: Pd/C (150 mg), 0.25 mL min<sup>-1</sup> of aqueous formic acid (0.5 M), 50 °C, 5 bar. (Right) Formic acid conversion as a function of time on stream at different temperatures. Reaction conditions: Pd/C (150 mg), aqueous formic acid (0.5 M), 5 bar. Flow rate and temperature set at: (black square) 0.25 mL min<sup>-1</sup>, 50 °C; (red circle) 0.5 mL min<sup>-1</sup>, 70 °C; (blue upwards triangle) 0.5 mL min<sup>-1</sup>, 90 °C; (pink downwards triangle) 0.85 mL min<sup>-1</sup>, 110 °C.

**Table 1.** Calculated TOF (Equation 2) and *k<sub>d</sub>* from kinetic curve of continuous formic acid decomposition at different temperature.

Entry	T /°C	TOF /min <sup>-1</sup>	<i>k<sub>d</sub></i> x 1000 /min <sup>-1</sup>
1	50	1500	31
2	70	2360	43
3	90	3540	59
4	110	5860	81

As expected, increasing the reaction temperature leads to a clear increase in catalytic activity, with the initial turnover frequency (TOF<sub>0</sub>) of Pd/C increasing from 1500 h<sup>-1</sup> at 50 °C, to 5860 h<sup>-1</sup> at 110 °C. Interestingly, a similar increase for  $k_d$  is also observed (from 0.031 to 0.081 between 50 and 110 °C, respectively), in a first instance suggesting a temperature dependence for deactivation (Table 1). However, to better evaluate the extent of deactivation and its temperature dependency, the time on stream data should be compared based on the number of reaction cycles performed, by re-plotting the data as relative performance (Equation 3) as a function of substrate turnover (Equation 4) (Figure 3 (Left)). In doing so, it can be seen that all points broadly converge on the same curve, with the partial exception of the highest temperature reaction (110 °C), which appears to deactivate very slightly faster per number of substrate turnovers than reaction at lower temperatures. This observation indicates that deactivation correlates better to the quantity of substrate that has passed over the catalyst rather than to temperature directly. Verification of this was achieved by performing reactions with different initial concentrations of formic acid (0.25, 0.5, 0.75 and 1 M) at 50 °C (Figure 3 (Right)). In this case, the relative performance of Pd/C is identical at all concentrations when compared at the same number of substrate turnovers. The correlation of deactivation to the number of substrate turnovers suggests deactivation may relate to a reaction-based stimulus, such as effects related to the reactant, product or by-product(s), or the deposition of residue, since solvothermal effects alone, such as sintering and/or lixiviation of the metal, would more likely correlate to temperature and time.

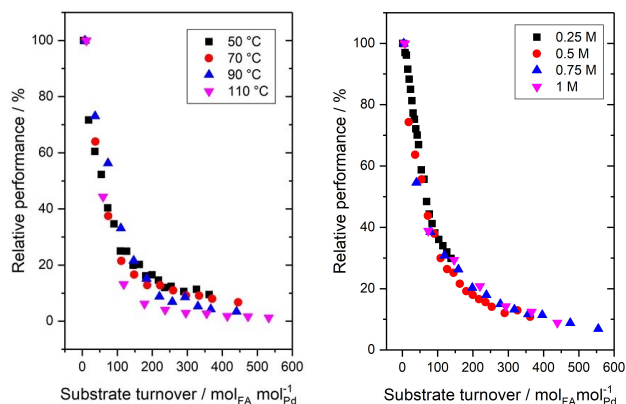


**Figure 3. (Left)** Effect of temperature on the relative performance of Pd/C as a function of substrate turnover. Reaction conditions: Pd/C (150 mg), aqueous formic acid (0.5 M), 5 bar. Flow rate and temperature set at: (black square) 0.25 mL min<sup>-1</sup>, 50 °C; (red circle) 0.5 mL min<sup>-1</sup>, 70 °C; (blue upwards triangle) 0.5 mL min<sup>-1</sup>, 90 °C; (pink downwards triangle) 0.85 mL min<sup>-1</sup>, 110 °C. **(Right)** Effect of formic acid concentration on the relative performance as function of substrate turnover during continuous formic acid decomposition. Reaction conditions: Pd/C (150 mg), 50 °C, 5 bar. Different aqueous formic acid concentration and flow rate: (black) 0.25 M and 0.12 mL min<sup>-1</sup>, (red) 0.5 M and 0.25 mL min<sup>-1</sup>, (blue) 0.75 M and 0.38 mL min<sup>-1</sup>, (pink) 1 M and 0.5 mL min<sup>-1</sup>.

To better understand the causes of deactivation, and identify how to prevent it from occurring, attempts to regenerate the catalyst were made. Other than having an obvious practical value, this also allows determination of whether deactivation is permanent or reversible, and provides an indirect way of studying the type of deactivation involved. We identified that regeneration of the catalyst could be achieved both by classical thermal treatment of the reactor bed (air flow, 20 °C min<sup>-1</sup>, 180 °C for 90 min), or by

flushing the deactivated catalyst in fresh solvent (pure water, 50 °C for 150 min). Figure 4 (Left) demonstrates that thermal regeneration of the catalyst completely restores its initial activity, whereas Figure 4 (Right) demonstrates how activity can be restored by washing the sample in water. Notably, the extent of regeneration achieved during washing in water strongly depends on the quantity of water passed over the used catalyst (ESI Figure S3). Notably, the rates of deactivation ( $k_d$ ) observed in both second cycles *i.e.* after thermal or washing regeneration, are unchanged to that exhibited by the fresh catalyst (0.027 min<sup>-1</sup>, 0.027 min<sup>-1</sup> and 0.026 min<sup>-1</sup>, respectively), indicating that the catalyst does not undergo permanent changes during reaction or regeneration. We note that spontaneous regeneration of the catalyst simply by removal from the reactor can be ruled by a control experiment performed by removing a spent catalyst from the reactor, leaving it to dry at room temperature overnight (16 h), and then re-examining its activity. This procedure resulted in no regeneration being observed. As such, it is clear that thermal treatment or washing is necessary for reactivation of the catalyst, and that the deactivated catalyst remains inactive upon removal from the reactor – an important consideration for further spectroscopic study.

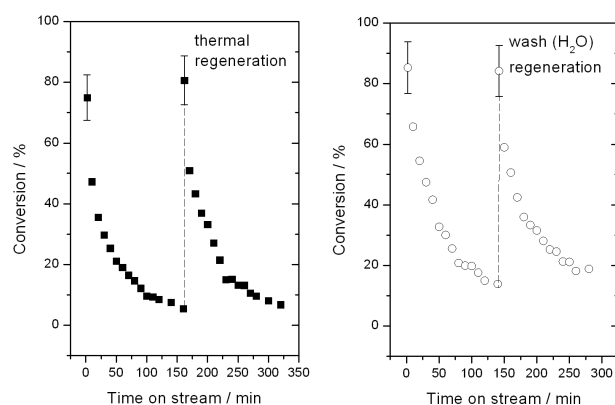


**Figure 4. (Left)** Formic acid conversion as function of time on stream of fresh and regenerated catalyst, regenerated by heating the reactor at 180 °C for 90 min in static air. **(Right)** Formic acid conversion as function of time on stream of fresh and regenerated catalyst regenerated by flushing the reactor with 2.5 mL min<sup>-1</sup> of water for 150 min at 50 °C. Reaction conditions: Pd/C (150 mg), 0.25 mL min<sup>-1</sup> of aqueous formic acid (0.5 M), 50 °C, 5 bar.

Spectroscopic studies, and generation of structure-activity-lifetime relationships. To better understand deactivation of the catalyst, and to propose methods to mitigate its impact, it is necessary to generate structure-activity-lifetime relationships through correlation of the kinetic observations to characterisation of the catalyst. Accordingly, a variety of techniques were used to study the physical and chemical nature of the catalyst and its active sites, and to follow their transformation during the course of the reaction (fresh and deactivated) and following regeneration (washing and thermal). Transmission electron microscopy (TEM) was first used to get an insight on the dimension and distribution of the Pd particles on the surface of carbon. TEM images (Figure 5) of the fresh (A), deactivated (B) and regenerated (C) catalysts all exhibit a comparable dispersion of Pd particles on the carbon surface. By analysis the distribution of particles dimensions, shown in Figure 5A-C, it can be seen that all the samples possess an average particle size of 3.2 nm, and rather narrow distributions.

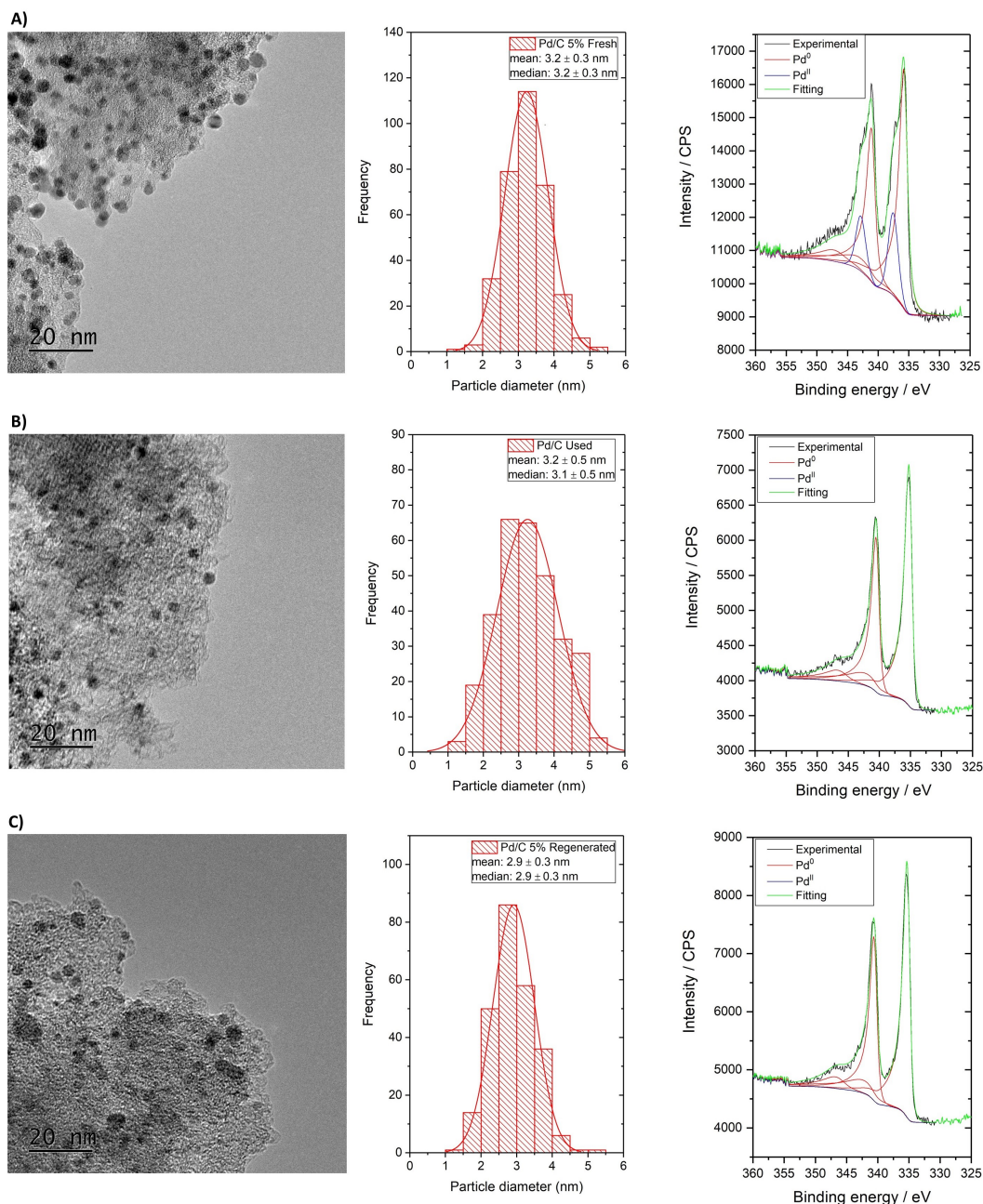


**Figure 5.** From left to right: TEM images, particle size distribution and XPS of Pd region of (top to bottom) (A) fresh, (B) used and (C) the catalyst regenerated by washing.

In fact, the degree of change in particle size and distribution following reaction, and later regeneration, is extremely modest, and likely points towards other factors being more dominant in respect to deactivation. To rule out that the slight changes in particle distribution between stages are due to leaching of specific size of Pd nanoparticles, elemental analysis was performed on the fresh and used catalysts. Given that the same amount of Pd was found in both samples, this indicates that an actual restructuring event occurs during reaction, as opposed to size-specific leaching (Table S1). The lack of extensive reorganisation of Pd is supported by ICP-MS analysis of the fresh and used catalysts (Table S1), which confirm that leaching of the active phase into the liquid phase does not occur, as indicated by the lack of change in Pd content of the catalysts during continuous operation.

**Table 2.** Parameters calculated from size distribution analysis from TEM, and the distribution of Pd species as calculated from XPS, for the fresh, used and water regenerated catalyst samples. A minimum of 300 particles was used for each analysis.

Entry	Sample	Mean / nm	Median / nm	Pd <sup>0</sup> / %	Pd <sup>II</sup> / %
1	Fresh	$3.2 \pm 0.3$	$3.2 \pm 0.3$	78	22
2	Used	$3.2 \pm 0.5$	$3.1 \pm 0.5$	100	0
3	Wash Regen	$2.9 \pm 0.3$	$2.9 \pm 0.3$	100	0

The types of Pd species present in the catalyst, and how they change during reaction and regeneration, was also investigated by X-ray Photoelectron Spectroscopy (XPS). XPS analysis, focused on the Pd(3d) region (Figure 5A-C), revealed two main peaks at 335.4 and 340.7 eV in the fresh, used and regenerated samples, corresponding to the Pd 3d<sub>5/2</sub> and Pd 3d<sub>3/2</sub> transitions, respectively. Deconvolution of these peaks allows the relative amount of Pd<sup>0</sup> and Pd<sup>II</sup> to be quantified. In line with previous studies, the fresh catalyst shows a mixed distribution of 78 % Pd<sup>0</sup>, and 22 % Pd<sup>II</sup>. After use in the PFR (Figure 6B, Table 2 Entry 2), only metallic Pd<sup>0</sup> is detected on the catalyst, likely due to reduction of the catalyst *in situ* by the hydrogen released as a product. In a first instance, the decrease of Pd<sup>II</sup> at the end of the reaction could be correlated to the loss of activity. However, no recovery of Pd<sup>II</sup> is observed even when the catalyst is fully regenerated. These observations strongly suggest that changes in the oxidation state of Pd do not correlate to catalytic performance. To verify this, and hence to study the effect of Pd oxidation state on catalytic activity, a series of pre-treatments were performed on the fresh catalyst prior to operation in the PFR. Specifically, the catalyst was treated in air (or 5 % hydrogen in argon) at 250 °C for 3 h, to oxidize (reduce) the nanoparticles prior to reaction. XPS analysis showed that during reduction, the percentage of Pd<sup>II</sup> decreased from 22 % in the untreated catalyst to 13 % (Figure S4 A, Table S2 Entries 1 and 3). The initial activity of this catalyst was found to be slightly higher (about 10% of increased initial activity), indicating that metallic Pd is the most active species, in line with previous reports (Figure S4 C). Unfortunately, the air treatment was not as effective, showing a modest increase in Pd<sup>II</sup> fraction from 22 to 25 %. As expected from this small change, no obvious changes in activity and stability can be detected. When combined, these studies indicate that deactivation of the catalyst cannot be attributed to the changes in Pd oxidation state observed during operation.

Another major cause of deactivation during heterogeneous catalysis is fouling, which relates to the deposition of residue on the catalyst surface and/or within its pores.<sup>44-47</sup> In such cases, deactivation is often related to the physical amount of reactant converted, and hence typically correlates with substrate turnover as opposed to time on stream, which could explain the preliminary kinetic analyses. Surface area and porosimetry analysis on the fresh catalyst revealed that the majority of the available surface area (1006 m<sup>2</sup> g<sup>-1</sup>) is microporous in nature (735 m<sup>2</sup> g<sup>-1</sup>), while only a smaller fraction of the area is mesoporous (Table 3, Entry 1). Since our kinetic protocol involves flushing the catalyst with water prior to introducing the substrate, and knowing that water can adsorb strongly on this type of support and may itself result in a significant loss of surface area, the sample flushed with water prior to switching to the feed solution was also measured. As can be seen (Table 3, Entry 2), a decrease of microporous area of 30 % compared to the untreated catalyst occurs simply due to start up of the reactor in water, prior to introduction of formic acid. For sake of further comparison, the porosity values of this sample are considered to be representative of the t<sub>0</sub> state of the catalyst. Following continuous operation, a dramatic decrease in the micropore area is observed, reducing by 92 % of the t<sub>0</sub> value. Clearly, deactivation of the catalyst is accompanied by a significant loss of micropore area. Since no dramatic changes to the structure of the used catalyst were observed either by Raman spectroscopy, XRD and evaluation of nitrogen isotherms (Figure S5-S7), it can be concluded that the loss of porosity relates to fouling and deposition, as opposed to structural conversion. To further verify a possible trend between deactivation and loss of micropore area, samples of Pd/C were further measured following partial (30 %, 80 %, Figure S3) regeneration by washing, and full regeneration by thermal treatment (Table 3, Entries 5-6). As can be seen, washing regeneration of the catalyst is accompanied by significant

restoration of microporous area, and the recovery of microporosity is even greater following thermal regeneration, likely due to the removal of the water molecules contributing to the initial loss of porosity at t<sub>0</sub>. These observations further indicate that deactivation and porosity may be related. However, it is notable that the recovery of porosity and the extent of regeneration by washing are not linearly correlated. In fact, whilst only 30 % of the activity is initially recovered after washing regeneration for 90 min at 1 mL min<sup>-1</sup>, around 75 % of the t<sub>0</sub> microporosity has been restored. Taken together, these experiments strongly indicate that surface area is a determining property for the activity of this material, and its loss is detrimental for activity. However, at least one other factor contributes to deactivation, and this event requires more extensive washing in water to be mitigated than loss of porosity alone.

**Table 3.** Surface area and porosimetry data obtained by nitrogen adsorption isotherm analysis. All values calculated by applying the DFT method to the nitrogen adsorption isotherms (77 K).

Entry	Sample	$S_{BET}$ /m <sup>2</sup> g <sup>-1</sup>	$S_{Micro}$ /m <sup>2</sup> g <sup>-1</sup>	$V_{Micro}$ /cm <sup>3</sup> g <sup>-1</sup>
1	Fresh	1006	735	0.28
2	Flushed in H <sub>2</sub> O (t <sub>0</sub> )	717	525	0.20
3	Used	171	42	0.01
4	Washed regen. 80%	707	517	0.20
5	Washed regen. 30%	584	412	0.15
6	Heated regen.	864	608	0.20

To understand the nature of the deposited material(s), and hence identify what species remain on the catalyst during reaction, a variety of experiments were performed on deactivated samples of Pd/C. Firstly, FTIR analysis of the fresh, used and washing regenerated catalysts was performed (ESI Figure S8). However, no signals that can be attributed to reaction residues were observed. Aliquots of the effluent produced during the washing regeneration procedure were also collected and analysed by <sup>1</sup>H NMR. However, the high degree of dilution resulted in no indicative signals being observed, even though calibration of the <sup>1</sup>H NMR for formic acid with an internal standard (tetramethylsilane) showed that the detectability limits to be of < 0.005 M. Accordingly, the gaseous effluent generated during thermal regeneration was monitored by mass spectrometry (akin to Temperature Programmed Oxidation Mass Spectrometry, TPO-MS, Figure 6). During thermal regeneration in air, only CO<sub>2</sub> was found to evolve from the deactivated catalyst. When compared to the fresh catalyst, it can be seen that the used sample evolves a much larger quantity of CO<sub>2</sub>. Moreover, the different evolution profiles also indicate that different species are present in the sample after reaction. The first signal of CO<sub>2</sub> evolving at 10 minutes is present both in the used and fresh catalyst, and may originate from the same species, albeit at a higher level of concentration in the used catalyst. However, major differences can be observed at later times. In particular, the used sample exhibits a well-defined evolution at 14.5 min, and a broader release at 15.5 min, while in the fresh sample these evolutions are absent and only a smaller, broader evolution is observed at 13.5 min.

Taken together, these analyses reveal that oxidisable carbonaceous material remains on the catalyst post-reaction, and that its removal is achieved at relatively low temperature in line with the facile thermal regeneration process identified. To further verify whether this carbonaceous residue is related to loss of activity, the TPO-MS profile of the catalyst regenerated by washing in water was monitored. As can be seen, the carbonaceous residue present on the used catalyst is no longer present on the catalyst washed by water (and which exhibits activity), indirectly verifying that the presence of this residue is related to loss of activity. Unfortunately, although washing regeneration clearly removes the carbonaceous residue, attempts to detect the residue in the effluent by washing in D<sub>2</sub>O prior to <sup>1</sup>H NMR analysis, were also unsuccessful (Figure S9), either indicating that i) the residual carbon is present below the detectability limit of the instrument, and/or ii) that the (re-)addition of a solvent allows the retained carbonaceous species to react over the catalyst. Based on the detectability limit of <sup>1</sup>H NMR, and the ability of the catalyst to operate at room temperature, we favour the final hypotheses as reasons for why no carbonaceous species can be extracted from the catalyst post reaction.

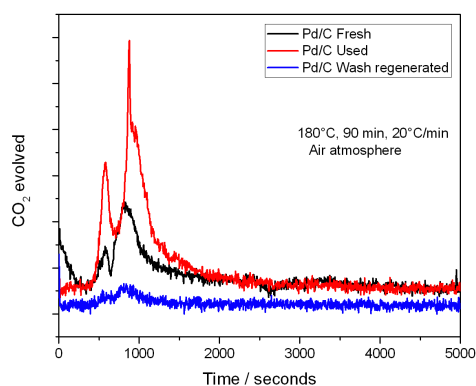


**Figure 6.** MS signal of CO<sub>2</sub> (M/Z = 44) evolved during heat treatment of used (red), fresh (black) and wash regenerated catalyst (blue). Conditions: air flow, 20 °C min<sup>-1</sup>, 180 °C for 3 h.

Although these studies do not provide direct identification of the residue(s) retained on the catalyst, they indicate that low molecular weight carbonaceous species that readily result in CO<sub>2</sub> formation in the presence of air must be retained on the catalyst. Since pore fouling is only partially responsible for deactivation (*Vide Supra*), these residues must also provide additional contributors to deactivation, most likely through active site poisoning.<sup>45-50</sup> Poison molecules can be the reactant and product, or by-products and impurities present in the feed. In each of these cases, poisoning often relates to the amount of reactant processed, and like fouling, thus often correlates to substrate turnover, in agreement to our kinetic data. Thus, to gain insight into the potential poisons present in the system, and hence indirectly to identify the residues present on the used catalyst, poisoning experiments were performed.<sup>40</sup>

The most likely poison molecules consistent with the TPD-MS analysis include CO, CO<sub>2</sub> and formic acid (or derivatives thereof), although the potential negative role of feed contaminants and other reaction products (H<sub>2</sub>) cannot be overlooked. To first verify the presence and role of feed contaminants, <sup>1</sup>H NMR was carried out on the formic acid solutions used for reaction. This revealed low, but non-negligible, concentrations of acetic and benzoic acid (Figure S10), which evidently may contribute to deactivation. However, utilising a distilled and purified solution of formic acid did not change the deactivation rate of the catalyst (*k<sub>d</sub>*), implying that the impurities present in the feed did not affect the catalyst performance under these experimental condi-

tions (Figure S11). In addition to impurities, reactants and products can also result in poisoning of the catalyst. In regards to poisoning by the products (H<sub>2</sub> and CO<sub>2</sub>, Figure 7), treatments in both H<sub>2</sub> atmosphere (5% H<sub>2</sub>/Ar atmosphere, 20 mL min<sup>-1</sup>, 250°C, 3h) and CO<sub>2</sub> (100% CO<sub>2</sub>, 20 mL min<sup>-1</sup>, 25°C, 3h) appeared to be slightly beneficial towards activity (Figure 7). Thus, poisoning by product molecules is unlikely to account for deactivation of the catalyst, and the carbonaceous residue present on the used catalyst is clearly not CO<sub>2</sub> itself.

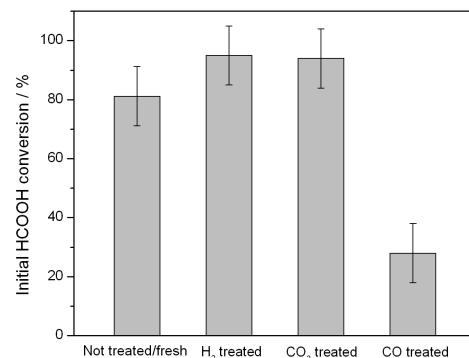


**Figure 7.** Initial activity of Pd/C for formic acid dehydrogenation following various pre-treatment procedures. H<sub>2</sub> treated: 5% H<sub>2</sub>/Ar atmosphere at 250°C, 20 mL min<sup>-1</sup>, 3 h, 5 °C min<sup>-1</sup>. CO<sub>2</sub> treated: flushed with 100% CO<sub>2</sub> (20 mL min<sup>-1</sup>) at 25°C, 3 h. CO treated: flushed with 10% CO - He (20 mL min<sup>-1</sup>) at 25°C, 3 h.

Many works in literature indicate that Pd nanoparticles-based catalysts are particularly susceptible to CO poisoning.<sup>48-51</sup> This is particularly relevant in this case, since competition between dehydrogenation (pathway 1, thermodynamically favoured) and dehydration (pathway 2) is present.



Gas composition analysis (GC-FID with methaniser unit) demonstrate that only trace amounts of CO are formed during this process, with a CO:CO<sub>2</sub> ratio of 1:100,000 being detected at 50 °C (ESI Figure S12). However, checking the susceptibility of the catalyst to CO poisoning is still of relevance during extended operation, where gradual accumulation and poisoning can occur. Accordingly, a fresh catalyst was packed into the reactor and treated in a flow of 10 % CO in helium (20 mL min<sup>-1</sup>) for 3 hours, after which time, the feed was switched to the reaction solution, and an otherwise-standard continuous flow reaction performed. As can be seen, the initial activity of the catalyst after CO poisoning is dramatically lower than the untreated catalyst, with an initial conversion of only 32 % achieved, compared to *ca.* 80 % value observed for the untreated sample (Figure 7). This result clearly indicates that CO is an effective poison of the catalyst. However, whilst washing regeneration is sufficient to restore full activity of the catalyst between typical reaction cycles (Figure 8, top), in the case of the CO-treated catalyst, washing only restores the additional amounts of activity lost during the reaction cycle itself *i.e.* washing regeneration does not restore activity to *ca.* 80 % conversion, and hence is not able to mitigate CO poisoning (Figure 8, bottom), in line with the non-poisoned catalyst. This strongly indicates that although CO is an effective poison of the catalyst, CO poisoning is not the reason behind loss of activity of Pd/C during the experiments performed in this study, since the mode(s) of deactivation observed during reaction are amenable to washing regeneration.

Although washing regeneration is unable to reverse CO poisoning, thermal regeneration is still feasible (180 °C, 90 min), with this treatment restoring the catalyst to its standard level of activity. Based on this, we can conclude that during the reaction, CO poisoning does not give the main contribution to deactivation, as demonstrated by the fact that the activity between cycles can be totally recovered by washing, while CO poisoning itself cannot be removed by simply washing the catalyst with water.

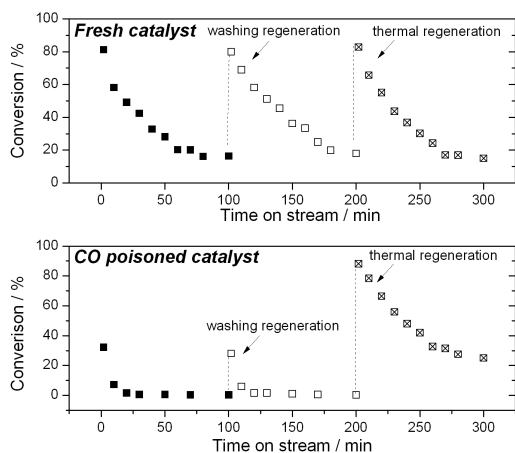


**Figure 8.** Formic acid dehydrogenation over Pd/C as (top) untreated catalyst, and (bottom) CO-poisoned catalyst. In the later, the reaction was started after treating the catalyst with a stream of CO (10 % of CO in He, 20 mL min<sup>-1</sup>, 3 hours). In both cases, washing regeneration was performed after 100 minutes (2.5 mL min<sup>-1</sup>, 150 min at 50 °C), and a thermal regeneration was performed prior to a third cycle by heating the reactor in static air at 180 °C for 90 min. Reaction conditions: Pd/C (150 mg), 0.25 mL min<sup>-1</sup> of aqueous formic acid (0.5 M), 50 °C, 5 bar.

In addition to impurities, by-products and products, poisoning by substrate is also possible. In fact, acids such as formic acid are well-established poisons for nanoparticle based catalysts, due to their ability to chelate strongly to the metal centres. In fixed bed reactors, deactivation events that are dependent on the concentration of reactants, such as fouling or poisoning, often involve specific parts of the catalyst bed, since the reactant concentration is space dependent rather than time dependent, as is the case of batch reactors. For instance, deactivation due to poisoning by formic acid would be more severe at the front of the catalyst bed, rather than at the end. Thus, to probe the deactivation of different parts of the reactor, a reaction was performed with a typical mass of catalyst (150 mg), but with the total amount of catalyst was split in two reactors placed in series. The reaction was initial run through the two reactor in series until the conversion of formic acid dropped from 95 to 70 %, when the reaction was paused and the two reactors separated. Subsequently, both “half” beds of catalysts were tested individually as two separate reactors, halving the flow rate in order to keep the contact time constant. If the catalytic bed had experienced homogeneous deactivation, the same value of initial activity would be found in both the reactors in the second part of the experiment. Instead, it is clear that the second (rear) catalyst bed exhibits much higher activity than the first (front) catalyst (Figure 9). The higher initial activity can be attributed to a lower degree of deactivation of the catalytic bed initially located in the rear half of the reactor, where the concentration of reactant is lower. Accordingly, since deactivation of the catalyst is dependent on both substrate turnover and space, and is worst at the beginning of the reactor bed, it is likely that deactivation of the catalyst occurs from an effect related to the presence of the reactant, rather than (by-)products. Notably, of all the species present in the reactor, only formic acid can also be responsible for pore

fouling, since the products and by-products of the reaction are all gaseous, and should readily be liberated from the catalyst. Poisoning by formic acid would also result in the evolution of CO<sub>2</sub>

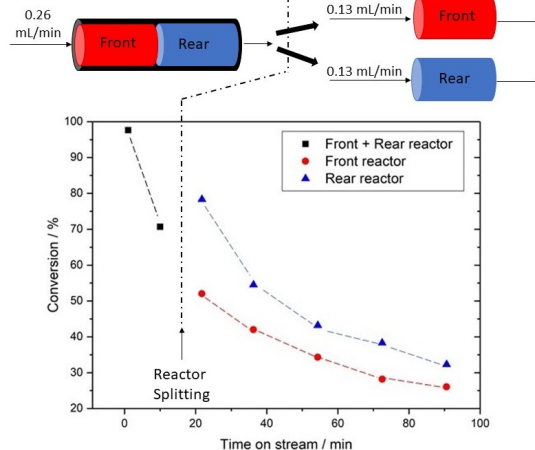


**Figure 9.** Performance of Pd/C for formic acid decomposition measured at different spaces of the catalytic bed. Reaction condition: first 10 min of reaction carried out with two reactors in series. Total amount of Pd/C 150 mg, 0.26 mL min<sup>-1</sup> of aqueous formic acid (0.5 M), 50 °C, 5 bar back pressure. After 10 min the reaction was stopped and the two reactors separated. The reaction was then continued in duplicate, with both “half” beds tested under otherwise identical condition: Pd/C (75 mg), 0.13 mL min<sup>-1</sup> of aqueous formic acid (0.5 M), 50 °C, 5 bar.

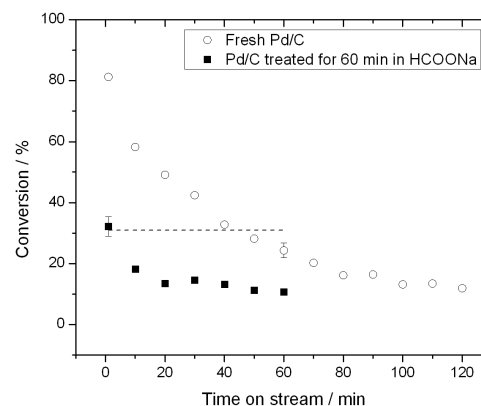


**Figure 10.** Performance of Pd/C for formic acid decomposition measured following pre-treatment in an aqueous solution of HCOONa (0.5M, 60 min, 0.25 mL min<sup>-1</sup>). Reaction conditions: Pd/C 150 mg, 0.25 mL min<sup>-1</sup> of aqueous formic acid (0.5 M), 50 °C, 5 bar back pressure.

In the case of formic acid, many theoretical reports on the mechanism suggest this reaction first involves deprotonation of formic acid on the surface of the metal, followed desorption of release of H<sub>2</sub> and CO<sub>2</sub>.<sup>38,52-53</sup> Formate anions possess a higher chelating strength than their protonated counterpart, making them possible candidate as a poisoning agent. To probe the possible influence of the formate anion, a reaction was performed following pre-treatment of the catalyst in an aqueous solution of sodium formate (Figure 10). We note that sodium formate itself does not result in the production of much H<sub>2</sub>, and hence allows the impact of products of the reaction on deactivation to be minimised. In this case, the initial conversion level of the catalyst after treatment for 60 minutes in aqueous sodium formate was consistent with that typically observed after 45-60 minutes on stream, confirming the formate anion is the genesis of poisoning in this system.

**Achieving continuous performance.** When combined, the spectroscopic, kinetic and mechanistic studies presented in this section clearly indicate that deactivation of the catalyst during the continuous conversion of formic acid to hydrogen relates to poisoning and fouling due to the presence of the substrate, formic acid. Since the substrate is an essential component of the reaction system, and it cannot necessarily be avoided during the reaction, this makes continuous operation of the system very challenging. With the aim of maximising durability of the system, and hence permitting true continuous operation to be achieved, we reasoned that continuous performance should be feasible by running in a Continuous Stirred Tank mode (CSTR), where the steady state concentration of formic acid can be minimised by operating the system at a level of conversion as close to 100 % as possible *i.e.* by matching the rate of formic acid conversion with the rate of formic acid addition, so that a steady state concentration of zero is achieved.

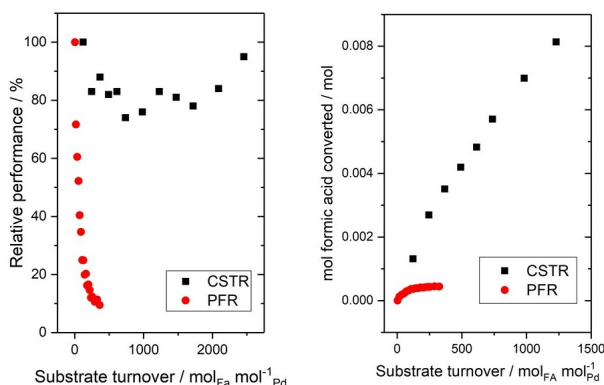


**Figure 11.** Comparison of Pd/C performance during formic acid dehydrogenation in CSTR and PFR. In particular, **(Left)** Relative performance of the catalyst as a function of substrate turnover, and **(Right)** cumulative moles of formic acid converted in the two systems as function of substrate turnover. CSTR reaction condition: Pd/C (45 mg), 0.01 mL min<sup>-1</sup> of pure formic acid, 60 mL of reactor volume, 50 °C, 800 rpm. PFR reaction conditions: Pd/C (150 mg), 0.25 mL min<sup>-1</sup> of aqueous formic acid (0.5 M), 50 °C, 5 bar back pressure.

To achieve this, pure formic acid was flown into a round bottom flask filled with 60 mL of water and the catalyst at 50 °C. Despite not reaching full conversion, the catalyst exhibited much higher levels of stability in the CSTR, with the relative activity of the catalyst after over 2000 turnovers comparable to its activity at  $t_0$  (Figure 11, Left). Notably, the  $k_d$  value of this reaction is 35-times lower than that of the best  $k_d$  value obtained in plug flow mode, demonstrating how the choice of reactor and conditions can remarkably improve catalyst stability. Because of its increased stability, more formic acid could be converted in CSTR than the PFR, as clearly shown in Figure 10 (Right). In light to the fact that the activity can be recovered by washing the catalytic bed with water, it can be hypothesised that in the CSTR, the constant stirring and the better dispersion of the catalyst in a higher volume of water account for a similar effect observed after washing, mitigating the deactivation of the catalyst. However, it should be added that despite the superior performance of the CSTR in terms of stability and overall productivity, the lower catalyst-to-volume ratio and the decreased steady state concentration of formic acid do compromise the initial space-time-yield of the reactor by an order of magnitude.

## Conclusions

The continuous additive-free production of formic acid at mild conditions was targeted over heterogeneous Pd/C. Although rapid rates of deactivation were initially encountered, structure-activity-lifetime relationships were developed, allowing deactivation to be attributed to side-effects associated with the substrate, formic acid. Based on these relationships, continuous operation could be achieved by operating in a CSTR mode, which allowed H<sub>2</sub> to be generated continuously for over 2000 turnovers without loss of activity by matching the rate of formic acid addition and consumption. Although the CSTR is characterised by lower rates of activity than the analogous PFR, the dramatic improvement in stability (35-fold) overall results in a more productive and favourable process for continued research.

## Experimental details

### Equations

- (1) Turnover frequency = TOF =  $\frac{n \text{ formic acid converted}}{n \text{ Pd} \times \text{time}}$
- (2) Contact time =  $\tau$  (min) =  $\frac{\text{Volume}_{(\text{catalyst bed})}}{\text{Flow rate}}$
- (3) Relative performance =  $\frac{\text{Conversion, } X(t)}{\text{Conversion, } X(t_0)} \times 100$
- (4) Substrate turnover =  $\frac{n(\text{formic Acid}) \text{ time}^{-1} \times \sum \text{time}}{n(\text{Pd})}$
- (5) Space-time-yield =  $n(\text{formic acid})L^{-1}(\text{reactor})h^{-1}$

### Materials

A commercial Pd (5 wt. %) supported on activated carbon was used as received (Merck-Sigma). Formic acid (98 % purity) was purchased on Merck-Sigma and used without any purification if not stated in the text. Sodium formate was purchased from Merck-Sigma and used without any purification. Dilution of reactants was made in deionised water.

### Analytical methods

HPLC analysis have been performed by means of an Agilent Infinity 1200 equipped with a Metacarb 87H and UV detector. Conditions: 60 °C, 0.35 mL min<sup>-1</sup>, 0.1 wt. % of H<sub>3</sub>PO<sub>4</sub> in water as eluent. <sup>1</sup>H NMR were acquired with a Bruker 500 MHz. Spectra are acquired with D<sub>2</sub>O as deuterated solvent and water suppression method is employed. Formic acid concentration have been determined by means of HPLC and <sup>1</sup>H NMR technique by extrapolate the value from calibration curves built with standard samples at known concentration. Succinic acid has been used as internal standard for the quantification of formic acid via HPLC. 0.3 mL aliquot of reaction mixture have been collected at different time on stream and diluted with 0.3 mL solution of 0.05 M succinic acid. <sup>1</sup>H NMR quantitative analysis have been performed by measuring the area of the formic acid signal at 8.1 ppm normalised with the area of a known concentration of tetramethylsilane (TMS). NMR sample have been made by mixing 0.7 mL of reaction aliquot and 0.1 mL of D<sub>2</sub>O and inserting a sealed capillary containing 0.1 mL of TMS.

Qualitative gas analysis have been performed on the gas collected in a tight-gas bag and injected into a Hiden mass spectrometer (QGC analyser).

### Kinetic studies

Multiple cycle of formic acid dehydrogenation reactions have been carried out in a round bottom flask loaded with 15 mg of Pd/C and 30 mL of water and stirred at 700 rpm with a magnetic

stirrer. Every cycle of reaction was initiated by adding 0.56 mL of formic acid (to have an initial aqueous formic acid concentration of 0.5 M) and the reaction was run approx. for 2 h until complete conversion. Afterwards, a fresh aliquot of formic acid was added and a new cycle started.

Continuous PFR formic acid dehydrogenation reactions were performed in a plug flow, stainless steel, tubular reactor. The reactor was connected to a Cole-Parmer HPLC pump in order to accurately regulate the reactant flow. The catalyst was densely packed into a 1/4" stainless steel tube (4.1 mm internal diameter) and held between two quartz wool plugs, and a frit of 0.5  $\mu\text{m}$  was placed at the reactor exit. The reactor was subsequently immersed in a thermostated oil bath at the desired reaction temperature. Pressure in the system was controlled by means of a backpressure regulator and a pressure of 5 bar at the end of the system was typically employed. Aliquots of the reaction solutions were taken periodically from a sampling valve placed after the reactor.

Periodic catalyst regeneration was performed heating the whole reactor in a combustion furnace (Carbolite MTF12/38/400) to 180 °C (20 °C min<sup>-1</sup>) in air (3 h).

CSTR formic acid dehydrogenation reactions were performed in a 100 mL two-necks round bottom flask. The flask was filled with 30 mL of DI water and 45 mg of Pd/C. the reaction temperature was controlled by submerging the flask in an oil bath thermostated at 50 °C, and the reaction mixture was stirred at 700 rpm by means of a magnetic stirrer bar. The two neck of the reactor where sealed by rubber septa. A Cole-Parmer HPLC pump dispensed pure formic acid into the flask at a flow rate of 0.01 mL min<sup>-1</sup>. The gas was collected into a gas bag and analysed at the MS spectrometer. Aliquot from the reaction mixture were collected and the concentration of formic acid analysed by means of HPLC.

### Kinetic studies

A PANalytical X'PertPRO X-ray diffractometer was employed for powder XRD analysis. A CuK $\alpha$  radiation source (40 kV and 30 mA) was utilised. Diffraction patterns were recorded between 10-80° 2 $\theta$  (step size 0.0167°, time/step = 150 s, total time = 1 h). TGA analysis was performed on a Perkin Elmer system. Samples were held isothermally at 35 °C for 10 minutes, before being heated to 600 °C (5 °C min<sup>-1</sup> ramp rate) in air. Elemental analysis on the solid have been performed by dissolving a weighted amount of material in *aqua regia* mixture and analysed by a Perkin Elmer inductively coupled plasma mass spectrometer (ICP-MS). Leaching of Pd from the fixed bed reactor have been checked by ICP-MS on the effluent collected at the outlet of the reactor. Samples for Transmission electron microscopy (TEM) analysis were dispersed as dry powder on a 300 mesh copper grid. Images were recorder with a JEOL JEM 2100 TEM model operating at 200 kV. X-ray photoelectron spectra (XPS) were recorded on a Kratos Axis Ultra DLD spectrometer using a monochromatic Al K $\alpha$  X-ray source. X-ray source (75-150 W) and analyser pass energies of 160 eV for survey scans, or 40 eV for detailed scans. Specific surface area and microporous volume were determined from nitrogen adsorption isotherms by using DFT method. Porosimetry measurements were performed on a Quantachrome Autosorb iQ2. Adsorption isotherms were obtained at 77 K. Raman measurement were obtain by means of a Renishaw spectrometer and using as light source a Laser light with 514 nm.

### ASSOCIATED CONTENT

Supplementary information, containing additional kinetic and spectroscopic details is available. The Supporting Information is

available free of charge as a PDF on the ACS Publications website.

### AUTHOR INFORMATION

#### Corresponding Author

E-mail: [hammond4@cardiff.ac.uk](mailto:hammond4@cardiff.ac.uk); Tel: +44 (0) 29 2087 6002

### ACKNOWLEDGMENTS

CH gratefully appreciates the support of The Royal Society, for provision of a University Research Fellowship (UF140207). CH and DP are grateful to The Royal Society for further research funding through the Grand Challenge Research Fund (CHGR1\170092).

### REFERENCES

#### REFERENCES

- (1) Park, S.; Vohs, J. M.; Gorte, R. J. Direct Oxidation of Hydrocarbons in a Solid-Oxide Fuel Cell. *Nature*. **2000**, 265–267.
- (2) Crabtree, G. W.; Dresselhaus, M. S.; Buchanan, M. V. The Hydrogen Economy. *Physics Today*. **2004**, 39-45.
- (3) Dunn, S. Hydrogen Futures. *International Journal of Hydrogen Energy*. **2002**, 235–264.
- (4) Baykara, S. Z. Hydrogen as Fuel: a Critical Technology? *Int. J. Hydrogen Energy*. **2005**, 545–553.
- (5) Dalebrook, A. F.; Gan, W.; Grasmann, M.; Moret, S.; Laurenczy G. Hydrogen Storage: Beyond Conventional Methods. *Chem. Commun.* **2013**, 8735-8751.
- (6) Christodoulou, C.; Karagiorgis, G.; Poullikkas A.; Lymberopoulos, N.; Varkarakis, E. A Review on Hydrogen Storage Technologies. *The Cyprus Journal of Science and Technology*, **2005**, 72-144.
- (7) Graetz, J. New Approaches to Hydrogen Storage. *Chem. Soc. Rev.* **2009**, 73–82.
- (8) Iulianelli, A.; Ribeirinha, P.; Mendes, A.; Basile, A.; Methanol Steam Reforming for Hydrogen Generation via Conventional and Membrane Reactors: A Review. *Renew Sustain. Energy Rev.* **2014**, 355–368.
- (9) Shen J.; Yang, L.; Hu, K.; Luo, W.; Cheng, G. Rh Nanoparticles Supported on Graphene as Efficient Catalyst for Hydrolytic Dehydrogenation of Amine Boranes for Chemical Hydrogen Storage. *Int. J. Hydrogen Energy*, **2015**, 1062–1070.
- (10) Nakamori, Y.; Kitahara, G.; Ninomiya, A.; Aoki, M.; Noritake, T.; Towata, S.; Orimo, S. Guidelines for Developing Amide-Based Hydrogen Storage Materials. *Mater Trans.* **2005**, 2093–2097.
- (11) Lu, Z. H.; Jiang, H. L.; Yadav, M.; Aranishi, K.; Xu, Q. Synergistic Catalysis of Au-Co@SiO<sub>2</sub> Nanospheres in Hydrolytic Dehydrogenation of Ammonia Borane for Chemical Hydrogen Storage. *J. Mater Chem.* **2012**, 5065–5071.
- (12) Wang Z.; Tonks, I.; Belli, J.; Jensen, C. M. Dehydrogenation of N-ethyl perHydrocarbazole Catalyzed by PCP Pincer Iridium Complexes: Evaluation of a Homogenous Borane Hydrogen Storage System. *J. Organomet Chem.* **2009**, 2854–2857.
- (13) Enthaler, S. Carbon Dioxide—The Hydrogen-Storage Material of the Future? *ChemSusChem*. **2008**, 801 – 804.
- (14) Jiang, H. L.; Singh, S. K.; Yan, J. M.; Zhang, X. B.; Xu, Q. Liquid-Phase Chemical Hydrogen Storage: Catalytic Hydrogen Generation Under Ambient Conditions. *ChemSusChem*, **2010**, 541 – 549.
- (15) Boddien, A.; Junge, H. Acidic Ideas for Hydrogen Storage. *Nat Nanotechnol.* **2011**, 265–266.
- (16) Loges, B.; Boddien, A.; Gartner, F.; Junge, H.; Beller, M. Catalytic Generation of Hydrogen from Formic Acid and its Derivatives: Useful Hydrogen Storage Materials. *Top Catal.* **2010**, 902–914.
- (17) Navarro, R. M.; Pena, M. A.; Fierro, J. L. G.; Hydrogen Production Reactions from Carbon Feedstocks: Fossil Fuels and Biomass. *Chem. Rev.* **2007**, 3952-3991.
- (18) Huber, G. W.; Iborra, S.; Corma, A. Synthesis of Transportation Fuels from Biomass: Chemistry, Catalysts, and Engineering. *Chem. Rev.*, **2006**, 4044–4098.

- (19) Hull, J.F.; Hameda, Y.; Wang, W. H.; Hashiguchi, B.; Periana, R.; Szalda, D. J.; Muckerman, J. T.; Fujita, E. Reversible Hydrogen Storage using CO<sub>2</sub> and a Proton-Switchable Iridium Catalyst in Aqueous Media Under Mild Temperatures and Pressures. *Nat. Chem.* **2012**, 383–388.
- (20) Loges, B.; Boddien, A.; Gartner, F.; Junge, H.; Beller, M. Iron-catalyzed Hydrogen Production from Formic Acid. *Top Catal.* **2010**, 902–914.
- (21) Loges, B.; Boddien, A.; Junge, H.; Beller, M. Controlled Generation of Hydrogen from Formic Acid Amine adducts at room temperature and Application in H<sub>2</sub>/O<sub>2</sub> Fuel Cells. *Angew. Chem. Int. Ed.* **2008**, 3962–3965.
- (22) Morris, D. J.; Clarkson, G. J.; Wills, M. Insights into Hydrogen Generation from Formic Acid using Ruthenium Complexes. *Organometallics.* **2009**, 4133–4140.
- (23) Boddien, A.; Mellmann, D.; Gärtner, F.; Jackstell, F.; Junge, H.; Dyson, P. J.; Laurency, G.; Ludwig R.; Beller, M. Efficient Dehydrogenation of Formic Acid using an Iron Catalyst. *Science.* **2011**, 1733–1736.
- (24) Fellay, C.; Dyson, P. J.; Laurency, G. A Viable Hydrogen Storage System based on Selective Formic Acid Decomposition with a Ruthenium Catalyst. *Angew. Chem. Int. Ed.* **2008**, 3966–3968.
- (25) Junge, H.; Boddien, A.; Capitta, F.; Loges, B.; Noyes, J. R.; Gladiali, S.; Beller, M.; Improved Hydrogen Generation from Formic Acid. *Tetrahedron Lett.* **2009**, 1603–1606.
- (26) Loges, B.; Boddien, A.; Junge, H.; Noyes, J. R.; Baumann, W.; Beller, M. Hydrogen Generation: Catalytic Acceleration and Control by Light. *Chem. Commun.* **2009**, 4185–4187.
- (27) Czaun, M.; Kothandaraman, J.; Goepfert, A.; Yang, B.; Greenberg, S.; May, R. B.; Olah, G. A.; Surya Prakash, G. K.; Iridium-Catalyzed Continuous Hydrogen Generation from Formic Acid and its Subsequent Utilization in a Fuel Cell: Toward a Carbon Neutral Chemical Energy Storage. *ACS Catal.* **2016**, 7475–7484.
- (28) Redondo, A. B.; Morel, F. L.; Ranocchiari, M.; Van Bokhoven, J. A. Functionalized Ruthenium–Phosphine Metal–Organic Framework for Continuous Vapor-Phase Dehydrogenation of Formic Acid. *ACS Catal.* **2015**, 7099–7103.
- (29) Martis, M.; Mori, K.; Fujiwara, K.; Ahn, W. S.; Yamashita, H. Amine-Functionalized MIL-125 with Imbedded Palladium Nanoparticles as an Efficient Catalyst for Dehydrogenation of Formic Acid at Ambient Temperature. *J. Phys. Chem. C.* **2013**, 22805–22810.
- (30) Bi, Q. Y.; Du, X. L.; Liu, Y. M.; Cao, Y.; He, H. Y.; Fan K. N.; Efficient Subnanometric Gold-Catalyzed Hydrogen Generation via Formic Acid Decomposition under Ambient Conditions. *J. Am. Chem. Soc.* **2012**, 8926–8933.
- (31) Grasmann, M.; Laurency, G. Formic Acid as a Hydrogen Source – Recent Developments and Future Trends. *Energy Environ. Sci.* **2012**, 8171–8181.
- (32) Zhang, X.; Llabrés i Xamena, F. X.; Corma, A. Gold(III) – Metal Organic Framework Bridges the Gap Between Homogeneous and Heterogeneous Gold Catalysts. *Journal of Catalysis*, **2009**, 155–160.
- (33) Gan, W.; Dyson, P. J.; Laurency, G. Heterogeneous Silica-Supported Ruthenium Phosphine Catalysts for Selective Formic Acid Decomposition. *ChemCatChem.* **2013**, 3124 – 3130.
- (34) Zacharska, M.; Podyacheva, O. Y.; Kibis, L. S.; Boronin, A. I.; Senkovskiy, B. V.; Gerasimov, E. Y.; Taran, O. P.; Ayusheev, A. B.; Parmon, V. N.; Leahy, J.J.; Bulushev, D. A.; Ruthenium Clusters on Carbon Nanofibers for Formic Acid Decomposition: Effect of Doping the Support with Nitrogen. *ChemCatChem.* **2015**, 2910–2917.
- (35) Zhou, X.; Huang, Y.; Xing, W.; Liu, C.; Liao, J.; Lu, T. High-Quality Hydrogen from the Catalyzed Decomposition of Formic Acid by Pd–Au/C and Pd–Ag/C. *Chem. Commun.* **2008**, 3540–3542.
- (36) Comotti, M.; Della Pina, C.; Matarrese, R.; Rossi, M. The Catalytic Activity of “Naked” Gold Particles. *Angew. Chem. Int. Ed.* **2004**, 5812–5815.
- (37) Gu, X.; Lu, Z. H.; Jiang, H. L.; Akita, T.; Xu, Q. Synergistic Catalysis of Metal–Organic Framework-Immobilized Au–Pd Nanoparticles in Dehydrogenation of Formic Acid for Chemical Hydrogen Storage. *J. Am. Chem. Soc.* **2011**, 11822–11825.
- (38) Sanchez, F.; Motta, D.; Roldan, A.; Hammond, C.; Villa, A.; Dimitratos, N. Hydrogen Generation from Additive-Free Formic Acid Decomposition Under Mild Conditions by Pd/C: Experimental and DFT Studies. *Topics in Catalysis*, **2018**, 254–266.
- (39) Scott, S. L.; A Matter of Life(time) and Death. *ACS Catal.* **2018**, 8597–8599.
- (40) Hammond, C. Intensification Studies of Heterogeneous Catalysts: Probing and Overcoming Catalyst Deactivation During Liquid Phase Operation. *Green Chem.* **2017**, 2711–2728.
- (41) Majewski, A.; Morris, D. J.; Kendall, K.; Wills, M. A Continuous-Flow Method for the Generation of Hydrogen from Formic Acid. *ChemSusChem.* **2010**, 431–434.
- (42) Sponholz, P.; Mellmann, D.; Junge, H.; Beller, M. Towards a Practical Setup for Hydrogen Production from Formic Acid. *ChemSusChem.* **2013**, 1172–1176.
- (43) Boddien, A.; Loges, B.; Junge, H.; Gartner F.; Noyes, J. N.; Beller, M.; Continuous Hydrogen Generation from Formic Acid: Highly Active and Stable Ruthenium Catalysts. *Adv. Synth. Catal.* **2009**, 2517–2520.
- (44) Padovan, D.; Botti, L.; Hammond, C. Active Site Hydration Governs the Stability of Sn-Beta during Continuous Glucose Conversion. *ACS Catal.* **2018**, 7131–7140.
- (45) Bartholomew, C. H. Mechanisms of Catalyst Deactivation. *Applied Catalysis*, **2001**, 17–60.
- (46) Zhang, L.; Seaton, N. A. Simulation of Catalyst Fouling at the Particle and Reactor Levels. *Chemical Engineering Science.* **1996**, 3257–3272.
- (47) Lange, J. P. Renewable Feedstocks: The Problem of Catalyst Deactivation and its Mitigation. *Angew.Chem.Int. Ed.* **2015**, 13186 – 13197.
- (48) Hu, C.; Ting, S. W.; Tsui, J. Chan, K. Y. Formic Acid Dehydrogenation Over PtRuBiO<sub>x</sub>/C Catalyst for Generation of CO-Free Hydrogen in a Continuous-Flow Reactor. *International journal of hydrogen energy.* **2012**, 6372–6380.
- (49) Lin, D.; , Shouzhong, Z. Enhanced Formic Acid Oxidation on Cu–Pd Nanoparticles. *Journal of Power Sources.* **2011**, 9369–9372.
- (50) Grunes, J.; Zhu, J.; Yang, M.; Somorjai, G. A. CO Poisoning of Ethylene Hydrogenation Over Pt Catalysts: a Comparison of Pt (111) Single Crystal and Pt Nanoparticle Activities. *Catalysis Letter.* **2003**, 157–161.
- (51) Liu, J.; Lucci, F. R.; Yang, M.; Lee, S.; Marcinkowski, M. D.; Therrien, A. J.; Williams, C. T.; Sykes, E. C. H.; Flytzani-Stephanopoulos M. Tackling CO Poisoning with Single-Atom Alloy Catalysts. *J. Am. Chem. Soc.* **2016**, 6396–6399.
- (52) Yingying, W.; Yuanyuan, Q.; Dongju, Z.; Chengbu, L. New Insight into the Decomposition Mechanism of Formic Acid on Pd(111): Competing Formation of CO<sub>2</sub> and CO. *The journal of physical chemistry.* **2014**, 2067–2076.
- (53) Herron, J. A.; Scaranto, J.; Ferrin, P.; Li, S.; Mavrikakis M. Trends in Formic Acid Decomposition on Model Transition Metal Surfaces: A Density Functional Theory study. *ACS Catal.* **2014**, 4434–4445.

## Table of contents graphic

